Ursolic Acid Suppresses Proliferation and Elicits Apoptosis of Laryngeal Carcinoma Cell HEp-2 through Activation of ROS Synthesis and Inhibition of Multiple Signaling Pathways

Shuya Wei (weishuya1011@126.com)
Wuhan Polytechnic
Nan Zheng
Wuhan Polytechnic

Research Article

Keywords: Ursolic acid, HEp-2, Antiproliferation, Apoptosis, ROS

Posted Date: April 8th, 2022

DOI: https://doi.org/10.21203/rs.3.rs-1532016/v1

Abstract

Laryngeal squamous cell carcinoma is one of the most common cancer-related causes of death worldwide. Thus, there is a constant need for improvement in drug development to promote treatment of this malignancy. In the present study, we identified a natural phytochemical, Ursolic acid, as a potent compound to counter laryngeal squamous cell carcinoma using HEp-2 cell line. Ursolic acid is capable of impeding proliferation and provoking apoptosis of HEp-2 cells. Interestingly, these anti-proliferative and proapoptotic effects is attributed to stimulation of ROS synthesis. In addition, we discovered that this UA-induced ROS stimulation is linked to the activation of MAPKs, PI3K/Akt, NF-κB and STAT3 signaling pathways. Our study characterized Ursolic acid as a potent anti-carcinoma drug with a multitargeting strategy, which enable it a novel and plausible treatment to laryngeal squamous cell carcinoma.

Introduction

Head and neck squamous cell carcinoma (HNSCC) is the sixth most common cancer worldwide (1). And laryngeal squamous cell carcinoma (LSCC) is one of the most common types of HNSCC, which also ranked the second most common in the United States (2). Risk factors for larynx cancers in the incidence and mortality vary in different parts of the world, yet are generally attributed to tobacco consumption, alcohol abuse, and infection with human papillomavirus (3). Contemporary management for these advanced malignancies is primarily total laryngectomy followed by adjuvant radiation therapy (4). Nevertheless, owing to the concurrent functional deficits and the incomplete clinical efficacy as to these treatments, there exists an unmet need for more therapeutic alternatives and reliable treatments for LSCC.

To date, researchers have obtained a growing interest in the effects of natural plant compounds in terms of cancer therapy. Because for a long time epidemiological studies have found that there is a strong correlation between health benefits and the intake of these phytochemicals derived from foods or medicinal herbs (5). In addition, researchers have provided substantial evidence of these natural compounds carrying anti-carcinogenic and free-radical scavenging properties (6). Most phytochemicals have been evaluated for their effects based on in vitro or in vivo studies before clinical stages. Some phytochemicals have already been utilized in clinical trials, such as Tamoxifen and Paclitaxel, which is widely used for treating primary breast cancer and various types of malignant diseases, respectively (7, 8).

Ursolic acid (UA), or 3-β-hydroxy-urs-12-en-28-oic acid (Fig. 1A), is a naturally synthesized pentacyclic triterpene acid, abundantly distributed in many fruits and vegetables (9). Data presented by previous studies have demonstrated that, similar to some phytochemicals that have been applied in clinical practice, Ursolic acid possess many pharmacologic benefit including anti-carcinogenic, anti-inflammatory, antioxidant capacities, etc. (9). For example, in a variety of cell-line based experiments, UA functioned as either an inhibitor to colorectal, lung and breast cancer cells (10–12) or a potentiator of oncolytic measles virotherapy against breast cancer cells (13). Notably, in addition to in vitro research, its nanoparticle were reported to suppress cervical tumors in a mouse xenograft mode (14). These studies laid ground work for

our understanding of the feasibility of UA as a cure for certain types of cancer. However, the effect of UA on LSCC has not been explored in previous work. Thus, in this work, we used an in vitro model to evaluate UA's capacity of fighting against laryngeal carcinoma. And here we report that UA carries a potent anti-proliferative and anti-carcinogenic ability against laryngeal cancer. We provide the proofs that UA prevents the growth of HEp-2 cells and induces apoptosis by promoting ROS level. We also unveiled that the mechanism of UA's effect against LSCC is a multitarget strategy that involves a series of signaling pathways, thereby providing the basis for discovering new natural compounds as effective treatment for cancer therapy.

Materials And Methods

Reagents and cell culture

Ursolic acid (purity > 98%) and dimethyl sulfoxide (purity > 98%) were purchased from Aladdin (Shanghai, China) and Sigma Aldrich (St. Louis, USA), respectively. UA powders were prepared as a 10 mg/ml stock solution in DMSO for in vitro experiments. On the day of use, the stock solutions were diluted in DMSO to the desired concentration.

Human larynx epidermoid carcinoma cells (HEp-2, ATCC, US) were cultured in Roswell Park Memorial Institute 1640 (RPMI-1640, Gibco, USA) containing 10% fetal bovine serum (FBS, Hyclone, USA) and 100 units/ml penicillin streptomycin (Gibco, USA). Cells were cultured under an atmosphere of 5% CO_2 at 37 ˚C in a humidified incubator. Before the drug treatment, cells were cultured in phenol red-free DMEM (Gibico) with 10% charcoal-stripped FBS (Biowest, Spain) for three days. Then, cells were switched to the fresh phenol red-free DMEM with 0.2% charcoal-stripped FBS and cultured for 24 hours.

Cell viability assay

Cell viability was analyzed by Cell Counting Kit-8 (CCK8, Beyotime, Shanghai, China) according to the manufacturer's protocols. Cells were seeded and cultured at a density of 5 × 103 /well in 100 µL of medium into 96-well microplates (Corning, USA). Then, the cells were treated with various concentrations of UA (0, 5, 10, 15, 20 and 25 µg/mL). After treatment for 24, 48 or 72 hours, 10 µL of CCK-8 reagent was added to each well and then cultured for 2 hours. All experiments were performed in triplicate. The absorbance was analyzed at 450 nm using a microplate reader (Bio-Rad, Hercules, CA, USA) using wells without cells as blanks. The proliferation of cells was expressed by the absorbance.

Clonogenic growth assay

HEp-2 cells in the logarithmic growth phase were prepared and pre-treated with indicated concentrations of UA or vehicle (DMSO) in 6-well plates for 24 or 48 h. Then prepare the agaroses: the 0.6%- and 1.2%-agaroses were dissolved in a 65°C water bath, and 0.5 mL 1.2% agarose was added to equal volume 2 × DMEM with 20% FBS and 2% P/S at 0.6% final-concentration. This DMEM-agarose mixture was immediately poured into another 6-well plates and cooled to the room temperature. Next, cell medium containing UA or vehicle were removed and cells were washed by PBS twice. 1000 treated cells per well

were rapidly suspended in equal volume 0.6%-agarose and immediately transferred onto the base agarose layer. After the agarose solidified, the plates were placed into an incubator at 37° C with 5% CO2 for 2 weeks and then stained with 0.5 mg/mL MTT. The numbers of colonies containing 50 cells or more were counted.

Cell cycle distribution analysis

HEp-2 cells were plated in 6-well plates and allowed to attach 24 h, and then treated with or without TC24 for 24 h. Only adherent cells were harvested and then washed twice with ice-cold PBS. Having been fixed gently in 4% paraformaldehyde (PFA) overnight at 4 ℃, cells were washed with ice-cold PBS twice. Then fixed cells incubated with 10% saponin and 1 mg/ml 2-phenylindole dihydrochloride (DAPI) in PBS at room temperature for 30 min. Cell cycle analysis was measured by a flow cytometer (Beckman Coulter, USA) with 10,000 events per sample and analysis by Flowjo software (Tree Star, OR).

Measurement of mitochondria membrane potential

Measurement of MMP were conducted using Mitochondrial Membrane Potential Assay Kit with JC-1 (Beyotime Biotechnology, China). For flow cytometry, cells were harvested and then stained with 10 μg/ml JC-1 at 37 ℃ for 20 min in a 5% CO2 humidifier incubator. After incubation, cells were washed twice with JC-1 staining buffer to remove the non-specific background staining. Then cells were detected by a flow cytometer (Beckman Coulter, USA) with 10,000 events per sample and analysis by Summit 4.3 software (Beckman Coulter, USA).

Cell apoptosis analysis

Cell apoptosis was tested with Annexin V-PE/7-AAD Apoptosis Detection Kit (Vazyme, China). The cells treated with vehicle or UA were stained using Annexin V and 7-amino-actinomycin according to the manufacturer's instructions. Then, samples were immediately analyzed using flow cytometry (Beckman Coulter, USA).

Measurement of Intracellular ROS

Intracellular ROS in HEp-2 cells were assayed using the dye 2,7-dichlorofuorescein diacetate (DCFH-DA, Sigma). For fow cytometry, cells were incubated with 10 μM DCFH-DA in serum and phenol-free medium at 37 ℃ in dark for 30 min. Cells were collected and washed twice with ice-cold PBS, and then were analyzed by flow cytometer mentioned above.

Western blot

Cells were washed twice with cold PBS, lysed in RIPA buffer (20 mM tris, pH 7.5, 150 mM NaCl, 1 mM EDTA, 1 mM EGTA, 1% v/v Triton X-100, 2.5 mM sodium pyrophosphate, 1 mM-glycerolphosphate, 1 mM Na3VO4, 1 mM NaF, 1 mM PMSF) at 4℃, and then sonicated for approximately 3 min. An aliquot of 20 μg of total protein was electrophoretically separated using 10% Tris-tricine gels and then transferred to PVDF membranes. Membranes were incubated overnight at 4℃ with indicated antibodies. The primary antibodies used include: anti-Bcl2, anti-Bax, anti-phospho-p65, anti-STAT, anti-phospho-STAT, anti-p38,

anti-phospho-p38, anti-ERK and anti-phospho-ERK (1:1000) from Cell Signaling Technology (USA), and anti-p65, anti-β-actin (1:3000), anti-p65, anti-Caspase3 (1:1000), anti-caspase9 (1:1000) were purchased from ABclone (Wuhan, China).

Statistical Analysis

All assays were repeated at least three times. Data shown are presented by means ± S.D. for at least one representative experiment. Statistical analysis was performed using one-way analysis of variance (ANOVA), followed by Bonferroni's ad *post-hoc* tests. *P*-value less than 0.05 was considered to indicate statistical significance.

Result

1. Ursolic acid inhibited the growth of HEp-2 cells

To investigate the role of Ursolic acid (Fig. 1A) in human laryngeal carcinoma, we introduced HEp-2 cell line as an in vitro model for following research. We firstly examined whether UA treatment is capable of impeding the growth HEp-2 cells. With CCK8 assay, we found UA reduced the amount of HEp-2 cells in a dose-depended manner after 24 h treatment (Fig. 1B). At the concentration of 25 μg/mL (5.47 μmol/L), the amount of living cells was reduced 43.09% ± 2.44% in UA-treated group compared to vehicle-treated control, and the half inhibitory concentration was around 20 μg/mL (4.38 μmol/L, 53.75% ± 1.11%). In the experiment that HEp-2 cells were incubated with UA for 48 h and 72 h, we observed similar trends of growth inhibition to Hep-2 cells in a dose-dependent manner (Supplementary data.1). Meanwhile, we employed chlorogenic growth assay to further examine if UA would show inhibition effect on the growth of HEp-2 cells in a longer period. Have being exposed to indicated concentrations of UA or vehicle for 24 or 48 h, MTT-stained HEp-2 cell clones in the agaroses were found lessened notably, as colony numbers of HEp-2 cells with UA treatment were reduced to 34.74% ± 2.41% of control at 24 h and 17.97% ± 3.71% at 48 h (Fig. 1C). These results suggest UA has a significant negative effect on HEp-2 cell growth.

To further investigate UA's blocking effect to cell proliferation, we tested UA's effect on cell cycle distribution of HEp-2 cells by flow cell cytometry. We also observed a dose-dependent changes in cell cycle distribution when indicated concentrations of UA was incubated with HEp-2 cells for 24 hours. As within the 20 μg/mL treated group, the proportion of G2/M phase cells shifts to (8.92% ± 0.53%) compared to control (24.06% ± 1.02%) (Fig. 1D). This result indicates that UA could inhibit the growth of HEp-2 cells via interfering with cell cycle progression. Together, above data unfolds the antiproliferation profile of UA on HEp-2 cells.

2. Ursolic acid induced apoptosis of HEp-2 cells

In addition to anti-proliferative effect, we investigated whether the cell viability of HEp-2 cells was also influenced by cell apoptosis of HEp-2 initiated by UA. It is well documented that a decline in the mitochondria membrane potential would induce a cascade of apoptotic pathway, hence a hallmark for early cell apoptosis (15). So, we first detected the alteration of this indicator by JC-1 staining and

subsequent flow cytometry analysis. Interestingly, we discovered only 20 μg/mL UA treatment increased the ratio of JC-1 aggregates over JC-1 monomers by 1.02-fold (Fig. 2A) compared with vehicle-treated control, whereas other concentrations of UA appeared to be insufficient to influence this index. Above all, this result still indicates the occurrence of early apoptosis of HEp-2 cells under maximum indicated concentration of UA.

Then, we assessed the UA's effect on the progression of apoptosis using Annexin V/7-ADD which stains cell membrane and intracellular DNA, respectively. The fluorescence was then measured by flow cytometry. Contrary to the data from JC-1 staining assay, UA treatment increased early apoptotic cells in a concentration-dependent manner (Fig. 2B). Among 20 μg/mL UA treated group, 40.85% ± 4.11 HEp-2 cells (early apoptotic 19.47% ± 5.09 and late apoptotic 21.38 ± 3.34, respectively) were in the apoptotic state. The data from both cytometry analysis demonstrate that HEp-2 cell apoptosis is attributed to UA treatment.

Meanwhile, it has been well established that lowering ratio of Bcl-2 (anti-apoptotic)/ Bax (pro-apoptotic) level and elevating cleavage of Caspase protein family marks the key events of intrinsic apoptosis progression (15). Therefore, we adopted Western Blot assay to further explore the molecular changes in HEp-2 cells during UA-induced apoptosis. We observed that Bcl-2 level was downregulated dose-dependently by UA treatment, while Bax level was up-regulated correspondingly. As to the change of Caspase protein, it was observed that UA treatment increased the amount of cleaved form of both Caspase3 and Caspase9 and in turn, decreased pro-cleaved form of both. Taken together, these data demonstrated that treatment of UA could lead to activation of intrinsic apoptosis pathway in HEp-2 cells.

3. UA increased ROS synthesis by inhibition of multiple signaling pathways in HEp-2 cells

UA's effect on growth inhibition and apoptosis activation has been noted in previous studies obtained in other cell lines. However, the descriptions of mechanism through which UA exerts these effects are not consistent among previous studies. The level of reactive oxygen species (ROS) has been established to have strong correlations with cell proliferation and apoptosis (16). We reason that the antiproliferative and apoptotic effect of UA mentioned in former results might also be ROS-mediated. So, using a cellular ROS assay kit, we measured the ROS level in UA-treated HEp-2 cells by flow cytometry analysis. It was found ROS level in 20 μg/mL UA-treated group was significantly higher (3.16 ± 0.29-fold) than control group (Fig. 3A). And this ROS elevation was in a concentration-dependent manner, which implies UA's stimulating effect on ROS production in HEp-2 cells.

Cellular ROS production was not regulated by a single mechanism (16). Therefore, to determine the underlying mechanism, we chose several canonical signaling pathway candidates including MAPKs, NF-κB, PI3K/Akt and STAT-JAK, and assayed the phosphorylation status of each pathway's key molecule in UA-treated HEp-2 cell lysates. Using Western Blot assay, we first checked MAPK pathway, which is comprised of ERK, p38 and JNK signaling. We discovered that three members of this pathway were all dephosphorylated under 20 ug/mL UA treatment, yet to distinct degree (Fig. 3B. p-ERK/t-ERK ,0.304 ±

0.097; p-JNK/ t-JNK, 0.477 ± 0.084; p-p38/t-p38, 0.223 ± 0.078-fold to control). Next, we detected UA's effect on other growth and apoptosis related signaling pathways. Phosphorylation level of PI3K/Akt was downregulated markedly under 20 ug/mL UA treatment (Fig. 3C, 0.395 ± 0.068-fold to control). STAT-JAK family member STAT3 was also dephosphorylated significantly (Fig. 3C, 0.293 ± 0.073-fold to control). For NF-κB signaling, phosphorylation level of its core component p65 was decreased to 0.408 ± 0.079-fold of control (Fig. 3C). Collectively, these results illustrate the mechanism of UA's effect on HEp-2 cells was related to activation of multiple signaling pathways, which mediates ROS-induced growth inhibition and cell apoptosis.

Discussion

Natural products have been recognized in therapeutic drugs for many years as an essential source of active substances. Among them, Ursolic acid has already been exhibited as a strong anti-carcinoma candidate by mounting evidence. Nevertheless, the effect of UA on LSCC remains uncovered. In this study, we thoroughly investigated UA's role in the activity of countering LSCC from two aspects in a laryngeal carcinoma cell line. On one hand, we discovered that Ursolic acid potently inhibited HEp-2 cell proliferation using cell viability assay and clonogenic growth assay. By cell viability assay, we find 20 μg/mL, or 4.38 μmol/L UA is sufficient to hinder cell growth of HegG2 by half. This concatenation is close to that of some clinical drugs like tamoxifen used in cell-line models (17). We further verified this anti-proliferating effect was via checking G2 and M phase arrest in cell cycle progression, which indicates a cellular molecular change at G2/M phase was implicated. This antiproliferative profile is also exemplified by Lin's (18) and Yang's (19) report. Moreover, Lin's team proved that suppression of Cyclin B1 could be the regulator of the cell cycle arrest caused by UA in colon adenocarcinoma cells (19).

On the other, we exploited multiple methods to investigate the apoptosis profile of HEp-2 cells. Apoptosis is regulated by two major pathways, the extrinsic pathway which is mediated by the transduction of extracellular death ligand signaling, and the intrinsic pathway, also referred to as the mitochondrial pathway, which is governed by a caspase cascade (20). And herein, we observed a substantial increase in Annexin V- or JC-1-stained positive cells, which demonstrates the flipped membrane during apoptosis occurred in HEp-2 cells that had been exposed to UA for 24 h. This cytometry data preliminarily confirmed UA induced apoptosis of HEp-2 through mitochondrial pathway. We further verified this mechanism by detecting primary molecules in intrinsic apoptosis pathway cascade. Intrinsic apoptosis cascade is mediated by antagonism between prosurvival and proapoptotic members of the Bcl-2 family and subsequent Capspase family (21). Our data showed treatment with UA decreased prosurvial Bcl-2 level and augmented proapoptotic Bax level. And this molecular change allowed downstream cleavage of the apoptotic initiator, Caspase3 and Caspase9 protein. Together, these data verified UA induces HEp-2 apoptosis via an intrinsic pathway.

In order to determine the molecular mechanism of UA on cell growth inhibition and apoptosis, we turned our interested into intracellular ROS level, which we believe is likely to be affected by the addition of UA, because ROS plays a pivotal role in mediating these two phenomena (16). We proved that ROS synthesis

was markedly stimulated by UA in HEp-2 cells. This finding is also exemplified in the work undertaken in other cells (22–24), indicating the elevation of ROS level induced by UA in vitro might be more common than expected. However, this finding is inconsistent with results from in vivo experiments, as Ursolic acid inhibits interactive NOX4/ROS in liver fibrosis mice (23), reduced ROS production stimulated by LPS in ApoE−/− mice (25) and ROS accumulation in C. elegans serotonin-deficient mutants (26). The controversy of UA's effect on ROS regulation between in vitro and in vivo data might be due to the difference of malignancy of the cell types and the diversity of pharmacokinetics process. More work needs to be done to explain the controversies found in vitro and in vivo models.

In addition, in attempt to identify the exact mechanism for the increase of ROS synthesis stimulated by UA in HEp-2 cells, we analyzed a class of typical signaling pathways such as ERK, JNK, p38, PI3K/Akt, NF-κB and STAT/JAK signaling, as they are all reported to mediate ROS-induced cell damage (27). Interestingly, we found that it is not a mere but all signaling pathways that are strongly impeded, which indicates the underlying mechanism is attributed to a strategy of multitarget inhibition. This theory can be evidenced by some previous findings. Kim reported that UA inhibits JAK2/STAT3 pathway in colorectal cancer cells (28). Prasad has long established UA inhibits JNK signaling (24). And Li found PI3K/Akt and NF-κB pathway was inhibited in vitro and in vivo respectively (25, 29). Besides, Park finds that Wnt/β-catenin is the mediator in the apoptosis in prostate cancer cells (30). Although above reports elaborated versatile mechanisms from various cellular signaling pathways, none of them analyzed the UA's antiproliferative and proapoptotic profile from a multitarget perspective. Yet our finding is consistent with Lin's work, which exhibits UA's multitarget feature in a cancer angiogenesis model (31). Given that these signaling pathways have extensive crosstalks to each other and interacts with other molecules as well (32), it is believed that a wider range of screening for signaling pathways is demanded to further verify the certain mechanism.

In conclusion, we characterized the natural-occurring compound Ursolic acid as a potent indictor to LSCC in HEp-2 cell model. Through a body of signaling activation and ROS stimulation, it suppresses LSCC cell growth and provokes LSCC apoptosis. We hold that this compound may be a promising candidate for clinical application, as its multitarget strategy represent a novel and effective approach to hinder LSCC.

Abbreviations

UA	Ursolic acid
LSCC	Laryngeal squamous cell carcinoma
ROS	Reactive oxygen species
MMP	Mitochondria membrane potential
MAPK	Mitogen-activated protein kinase
ERK	Extracellular regulated protein kinase
JNK	c-Jun N-terminal kinase
NF-κB	Nuclear factor kappa-B
STAT3	Signal transducer and activator of transcription 3

Declarations

Acknowledgement

This study was supported by Science and Technology Research Program（B2016581）of Hubei Provincial Department of Education.This study was also supported by Science and Technology Research Program (B2018456) of Hubei Provincial Department of Education.

Conflict of interest

The authors declare that they have no conflict of interest.

References

1. Caponio VCA, Troiano G, Adipietro I, Zhurakivska K, Arena C, Mangieri D, et al. Computational analysis of TP53 mutational landscape unveils key prognostic signatures and distinct pathobiological pathways in head and neck squamous cell cancer. British journal of cancer. 2020;123(8):1302–14.
2. Baird BJ, Sung CK, Beadle BM, Divi V. Treatment of early-stage laryngeal cancer: a comparison of treatment options. Oral Oncology. 2018;87:8–16.
3. Johnson DE, Burtness B, Leemans CR, Lui VWY, Bauman JE, Grandis JR. Head and neck squamous cell carcinoma. Nature reviews Disease primers. 2020;6(1):1–22.
4. Ali J, Sabiha B, Jan HU, Haider SA, Khan AA, Ali SS. Genetic etiology of oral cancer. Oral oncology. 2017;70:23–8.
5. Rodrigues T, Reker D, Schneider P, Schneider G. Counting on natural products for drug design. Nature chemistry. 2016;8(6):531–41.

6. Deng S, Shanmugam MK, Kumar AP, Yap CT, Sethi G, Bishayee A. Targeting autophagy using natural compounds for cancer prevention and therapy. Cancer. 2019;125(8):1228–46.
7. Zhu L, Chen L. Progress in research on paclitaxel and tumor immunotherapy. Cellular & molecular biology letters. 2019;24(1):1–11.
8. Ahmad I. Tamoxifen a pioneering drug: An update on the therapeutic potential of tamoxifen derivatives. European journal of medicinal chemistry. 2018;143:515–31.
9. Mlala S, Oyedeji AO, Gondwe M, Oyedeji OO. Ursolic acid and its derivatives as bioactive agents. Molecules. 2019;24(15):2751.
10. Wang X, Wang T, Yi F, Duan C, Wanwg Q, He N, et al. Ursolic acid inhibits tumor growth via epithelial-to-mesenchymal transition in colorectal cancer cells. Biological and Pharmaceutical Bulletin. 2019;42(5):685–91.
11. Wu J, Zhao S, Tang Q, Zheng F, Chen Y, Yang L, et al. Activation of SAPK/JNK mediated the inhibition and reciprocal interaction of DNA methyltransferase 1 and EZH2 by ursolic acid in human lung cancer cells. Journal of Experimental & Clinical Cancer Research. 2015;34(1):1–11.
12. Luo J, Hu YL, Wang H. Ursolic acid inhibits breast cancer growth by inhibiting proliferation, inducing autophagy and apoptosis, and suppressing inflammatory responses via the PI3K/AKT and NF–κB signaling pathways in vitro. Experimental and therapeutic medicine. 2017;14(4):3623–31.
13. Liu C-H, Wong SH, Tai C-J, Tai C-J, Pan Y-C, Hsu H-Y, et al. Ursolic acid and its nanoparticles are potentiators of oncolytic measles virotherapy against breast cancer cells. Cancers. 2021;13(1):136.
14. Wang S, Meng X, Dong Y. Ursolic acid nanoparticles inhibit cervical cancer growth in vitro and in vivo via apoptosis induction. International journal of oncology. 2017;50(4):1330–40.
15. Peña-Blanco A, García-Sáez AJ. Bax, Bak and beyond—mitochondrial performance in apoptosis. The FEBS journal. 2018;285(3):416–31.
16. Aggarwal V, Tuli HS, Varol A, Thakral F, Yerer MB, Sak K, et al. Role of reactive oxygen species in cancer progression: molecular mechanisms and recent advancements. Biomolecules. 2019;9(11):735.
17. Wang X, Chen Q, Huang X, Zou F, Fu Z, Chen Y, et al. Effects of 17β-estradiol and tamoxifen on gastric cancer cell proliferation and apoptosis and ER-α36 expression. Oncology letters. 2017;13(1):57–62.
18. Lin W, Ye H. Anticancer activity of ursolic acid on human ovarian cancer cells via ROS and MMP mediated apoptosis, cell cycle arrest and downregulation of PI3K/AKT pathway. J BUON. 2020;25(2):750–56.
19. Yang M, Hu C, Cao Y, Liang W, Yang X, Xiao T. Ursolic Acid Regulates Cell Cycle and Proliferation in Colon Adenocarcinoma by Suppressing Cyclin B1. Frontiers in pharmacology. 2021;11:2261.
20. Elango R, Athinarayanan J, Subbarayan VP, Lei DK, Alshatwi AA. Hesperetin induces an apoptosis-triggered extrinsic pathway and a p53-independent pathway in human lung cancer H522 cells. Journal of Asian natural products research. 2018;20(6):559–69.

21. Zhang Y, Yang X, Ge X, Zhang F. Puerarin attenuates neurological deficits via Bcl-2/Bax/cleaved caspase-3 and Sirt3/SOD2 apoptotic pathways in subarachnoid hemorrhage mice. Biomedicine & Pharmacotherapy. 2019;109:726–33.
22. Gan D, Zhang W, Huang C, Chen J, He W, Wang A, et al. Ursolic acid ameliorates CCl4-induced liver fibrosis through the NOXs/ROS pathway. Journal of cellular physiology. 2018;233(10):6799–813.
23. Wan S, Luo F, Huang C, Liu C, Luo Q, Zhu X. Ursolic acid reverses liver fibrosis by inhibiting interactive NOX4/ROS and RhoA/ROCK1 signalling pathways. Aging (Albany NY). 2020;12(11):10614.
24. Prasad S, Yadav VR, Kannappan R, Aggarwal BB. Ursolic acid, a pentacyclin triterpene, potentiates TRAIL-induced apoptosis through p53-independent up-regulation of death receptors: evidence for the role of reactive oxygen species and JNK. Journal of Biological Chemistry. 2011;286(7):5546–57.
25. Li Q, Zhao W, Zeng X, Hao Z. Ursolic acid attenuates atherosclerosis in ApoE−/− mice: role of LOX-1 mediated by ROS/NF-κB pathway. Molecules. 2018;23(5):1101.
26. Naß J, Abdelfatah S, Efferth T. Ursolic acid enhances stress resistance, reduces ROS accumulation and prolongs life span in C. elegans serotonin-deficient mutants. Food & Function. 2021;12(5):2242–56.
27. Liu Z, Huang Y, Jiao Y, Chen Q, Wu D, Yu P, et al. Polystyrene nanoplastic induces ROS production and affects the MAPK-HIF-1/NFkB-mediated antioxidant system in Daphnia pulex. aquatic toxicology. 2020;220:105420.
28. Kim K, Shin EA, Jung JH, Park JE, Kim DS, Shim BS, et al. Ursolic acid induces apoptosis in colorectal cancer cells partially via upregulation of MicroRNA-4500 and inhibition of JAK2/STAT3 phosphorylation. International journal of molecular sciences. 2019;20(1):114.
29. Li T, Zhang L, Jin C, Xiong Y, Cheng Y-Y, Chen K. Pomegranate flower extract bidirectionally regulates the proliferation, differentiation and apoptosis of 3T3-L1 cells through regulation of PPARγ expression mediated by PI3K-AKT signaling pathway. Biomedicine & Pharmacotherapy. 2020;131:110769.
30. Park J-H, Kwon H-Y, Sohn EJ, Kim KA, Kim B, Jeong S-J, et al. Inhibition of Wnt/β-catenin signaling mediates ursolic acid-induced apoptosis in PC-3 prostate cancer cells. Pharmacological reports. 2013;65(5):1366–74.
31. Lin J, Chen Y, Wei L, Hong Z, Sferra TJ, Peng J. Ursolic acid inhibits colorectal cancer angiogenesis through suppression of multiple signaling pathways. International journal of oncology. 2013;43(5):1666–74.
32. Rendra E, Riabov V, Mossel DM, Sevastyanova T, Harmsen MC, Kzhyshkowska J. Reactive oxygen species (ROS) in macrophage activation and function in diabetes. Immunobiology. 2019;224(2):242–53.

Figures

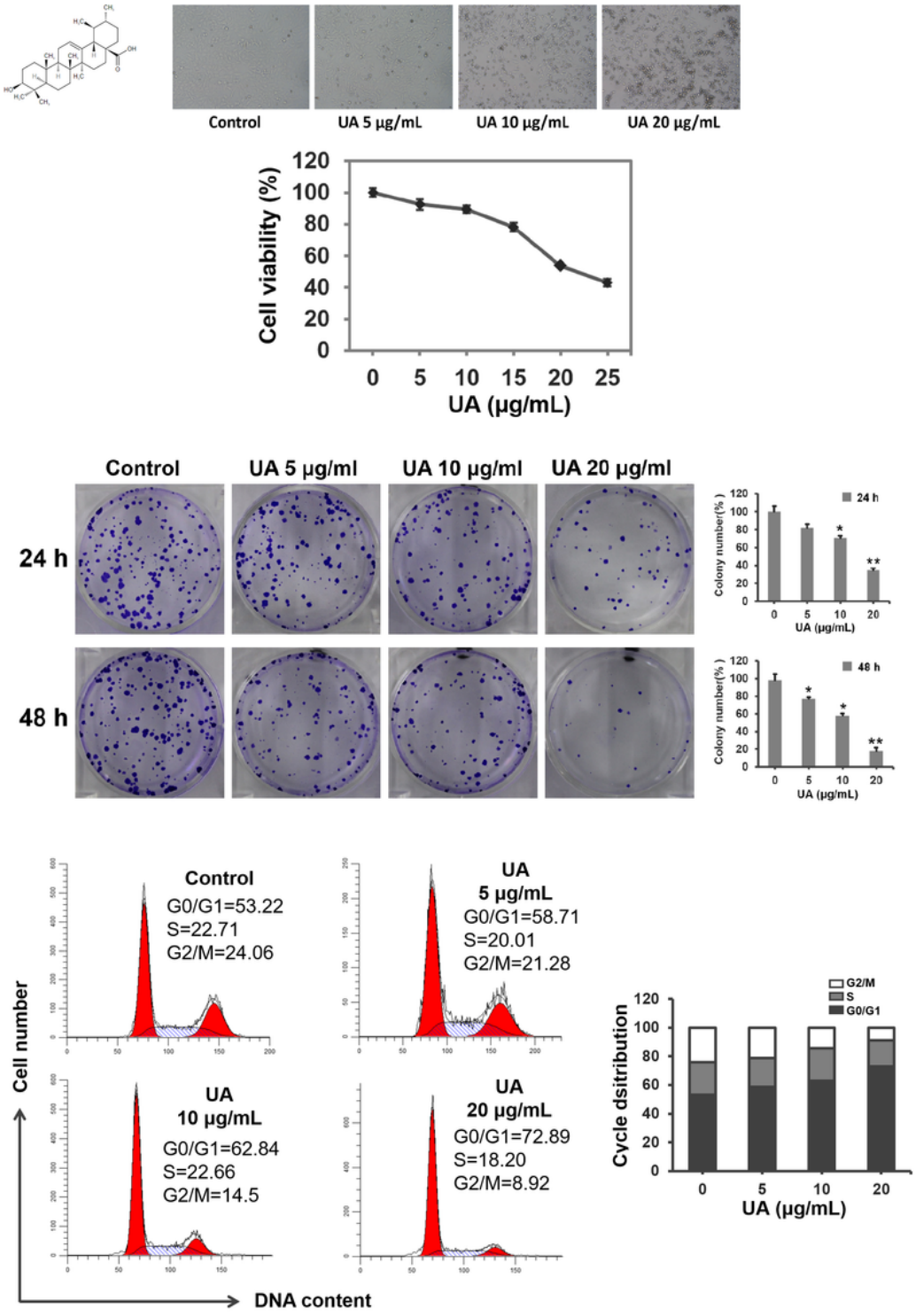

Figure 1

Ursolic acid inhibited the growth of HEp-2 cells. (A) Chemical structure of Ursolic acid. (B) CCK8 assay for UA's effect on HEp-2 cell viability. HEp-2 cells were incubated with DMSO or indicated concentrations of UA for 24 h and then stained with CCK8 The absorbance was read at 450 nm by a microplate reader. (C) HEp-2 cells seeded to 6-well plates and incubated with DMSO or indicated concentrations of UA for 24 h or 48 h. weeks, and then transferred to agarose for 2 more weeks' culture. Having being stained with MTT,

the plates were captured using a camera. (D) HEp-2 cells were treated indicated concentrations of UA for 24 h and then fixed with paraformaldehyde. Fixed cells were stained by DAPI and analyzed by flow cytometer. Histogram shows cell proportion of different cell cycle phases. All above assays were performed in triplicate. Results represent the mean ± S.D. from three independent experiments. Differences with *P < 0.05 and **P < 0.01 are considered statistically different and significant.

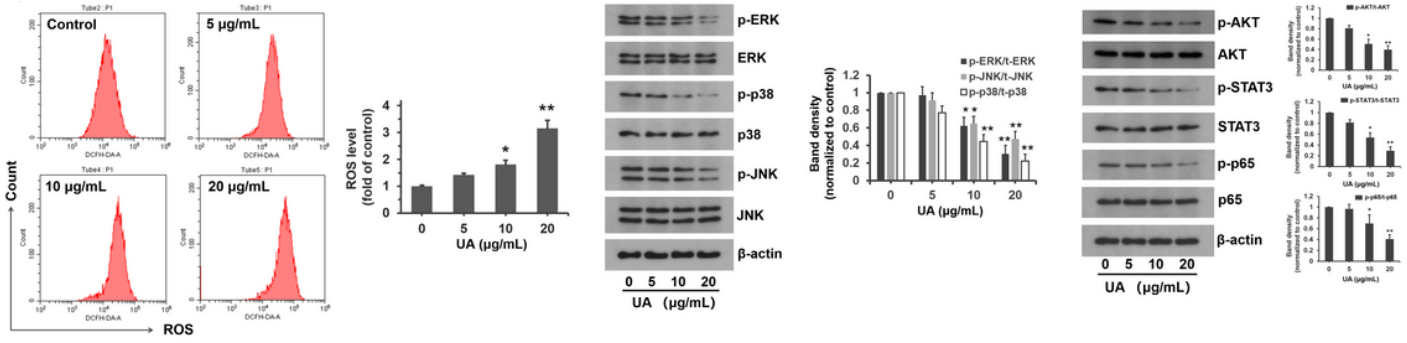

Figure 2

Ursolic acid promoted apoptosis of HEp-2 cells. HEp-2 cells were treated with DMSO or indicated concentrations of UA for 24 h in all following experiments. (A) After treated with UA, HEp-2 cells were harvested and then stained with 10 μg/ml JC-1. Measurement of mitochondria membrane potential was determined by early apoptotic cell amount measured by flow cytometer. (B). HEp-2 cells were harvested and then stained using an Annexin V-APC/7-ADD kit. The total amount of early and late apoptotic cells was measured by flow cytometer. (C) HEp-2 cells were harvested, lysed, and then subjected to Western Blot. β-actin was used as the internal control. Histograms shown were quantification to each assay. All above assays were performed in triplicate. Results represent the mean ± S.D. from three independent experiments. Differences with *P < 0.05 and **P < 0.01 are considered statistically different and significant.

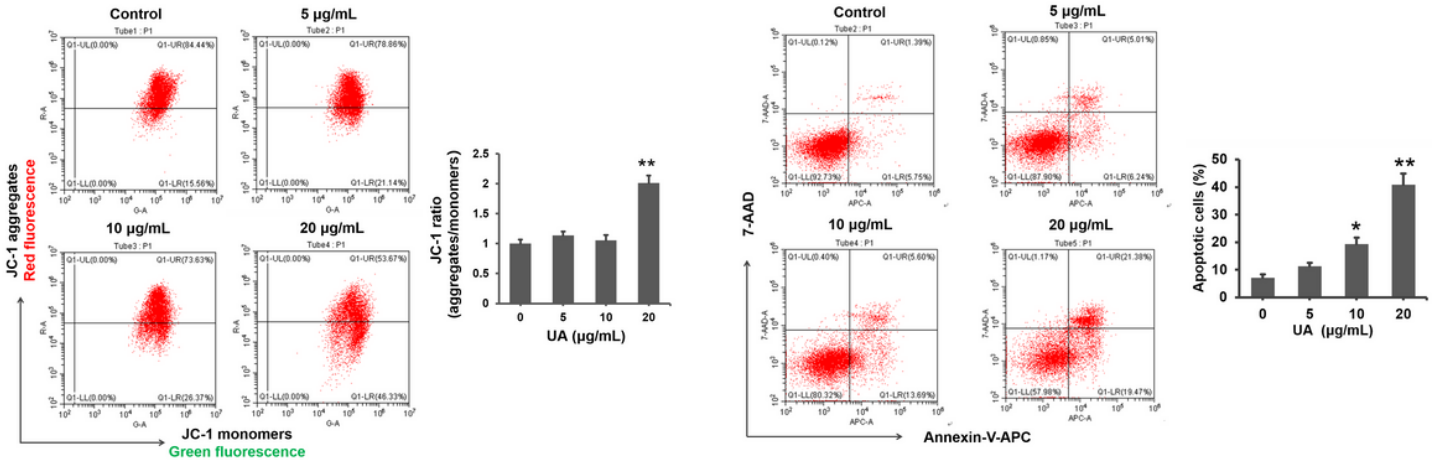

Figure 3

ROS production and cell signaling were affected by Ursolic acid. HEp-2 cells were treated with DMSO or indicated concentrations of UA for 24 h in all following experiments. (A) HEp-2 cells were incubated with 10 μM DCFH-DA in serum for 30 min and then collected for measurement of intracellular ROS using flow cytometer. (B) MAPK signaling was inhibited by UA. After UA treatment, HEp-2 cells were harvested and lysed. The amount of phosphorylated and total ERK, p38 and JNK was measured by Western Blot. β-actin was used as the internal control. (D) NF-κB and STAT-JAK signaling was inhibited by UA. The amount of phosphorylated and total STAT3 and p65 was measured by Western Blot. The western blots are representative of at least three independent experiments. Histograms were shown as the mean ± S.D. of at least 3 independent experiments. Differences with *P < 0.05 and **P < 0.01 are considered statistically different and significant.

Supplementary Files

This is a list of supplementary files associated with this preprint. Click to download.

- Sup.1.tif